

Sonomaglev: combining acoustic and diamagnetic levitation

George Hunter-Brown,¹ Naresh Sampara,¹ Matthew M. Scase,² and Richard J. A. Hill¹

¹*School of Physics and Astronomy, University of Nottingham, Nottingham NG7 2RD,*

UK

²*School of Mathematical Sciences, University of Nottingham, Nottingham NG7 2RD,*

UK

(*Electronic mail: george.hunter-brown@nottingham.ac.uk)

(Dated: 19 December 2022)

Acoustic levitation and diamagnetic levitation are experimental methods that both enable the contact-free study of liquid droplets and solid particles. Here we combine techniques of both into a single system that takes advantage of the strengths of each, allowing for the manipulation of levitated spherical water droplets (30 nL–14 μ L) under conditions akin to weightlessness, in the laboratory, using a superconducting magnet fitted with two low-power ultrasonic transducers. We show that multiple droplets, arranged horizontally along a line, can be stably levitated with this system and demonstrate controlled contactless coalescence of two droplets. Numerical simulation of the magnetogravitational and acoustic potential reproduces the multiple stable equilibrium points observed in our experiments.

Contactless manipulation has become an area of increased study over the last 10 years. New experimental techniques have been developed in a wide variety of disciplines, including: analytical chemistry^{1–6}, material sciences⁷, pharmacy^{8,9} and micro-assembly^{10–13}. Many contactless manipulation experiments rely upon a family of techniques classified as acoustic levitation. Acoustic levitation uses ultrasonic transducers to create a pressure field that applies acoustic radiation forces to suspend objects in a gaseous medium¹⁴. It has been shown that intricate, readily tuneable pressure fields can be constructed by using an array of small ultrasonic transducers^{15,16}, allowing for manipulation of multiple objects in three dimensions. The discovery that an array of ultrasonic transducers can create customisable acoustic levitation systems has led to a resurgence in the study of non-contact manipulation using acoustic levitation techniques^{17–20}.

In addition to these and other attractive features of acoustic levitation²¹, the method also has some drawbacks. From the earliest experiments, acoustically-levitated objects were observed to have a tendency to oscillate, attributed to the response of the acoustic field to the presence of the object^{22,23}. Objects may also start to rotate spontaneously due to streaming flows in the surrounding gas generated by the high pressure sound waves^{24,25}, though techniques to mitigate these effects and control the rotation have been demonstrated recently^{26,27}. These same streaming flows may also be problematic in studies of liquid droplets, where the air flow affects heat and mass transfer non-uniformly at the droplet's surface²⁸ and also sets up flows within the droplet²⁹. Acoustically-levitated liquid droplets are often deformed into oblate-like shapes^{30,31}; this typically occurs when the diameter of the droplet is of the same order as the acoustic wavelength. These characteristics, which are usually undesirable (though occasionally exploited³¹), are avoided in similar experiments using diamagnetic levitation (e.g. Ref. 32). Diamagnetic materials experience a repulsive force when placed in a static, spatially-varying magnetic field. A wide variety of solids and liquids, including water and organic material (including biological), can be levitated in a magnetic field of sufficient

strength and gradient (e.g. Refs. 33–40); typically a field of order 10 T is required, though levitation of graphite can be achieved using much weaker fields (e.g. Ref. 41). In contrast to the oscillating surface forces applied in acoustic levitation, diamagnetic levitation applies a constant body force that counteracts the force of gravity throughout the levitated object at the molecular level, and so closely mimics the weightless conditions on board an orbital or parabolic flight, or in a drop tower. Diamagnetically-levitated liquid droplets attain a spherical shape, due to the fact that surface tension forces dominate over the residual net body forces (~ 0.01 g) that stabilize the levitation.

On the other hand, the options to manipulate multiple objects magnetically are limited. Diamagnetic levitation allows for the levitation of multiple spatially-separated objects simultaneously if the objects have unique ratios of magnetic susceptibility to density. This differs from acoustic levitation where multiple acoustic 'traps' can be created for a particular material by manipulating the acoustic field. The creation of multiple traps for a single material is also possible using diamagnetic levitation, by manipulating the shape of the strong magnetic field, but this is technically more challenging than manipulating an acoustic field and correspondingly more restrictive.

In this letter, we demonstrate combining techniques from both acoustic and diamagnetic levitation to manipulate the position of liquid droplets, drawing on the strengths of each method. The force of gravity is compensated throughout the droplets by applying a vertical diamagnetic body force using a superconducting magnet, providing a simulation of weightlessness. Then, acoustic radiation forces are used to position the droplets. Since diamagnetic rather than acoustic forces provide gravity compensation in this case, the acoustic power required in these experiments is much smaller than that of a purely acoustic levitator. We further show that it is possible to reproduce the locations of the levitated droplets in simulations, calculating the magnetic and acoustic fields. Acoustic levitation has been combined with magnetic fields before, to study active matter levitated in liquids, but in those studies the magnetic field was used to provide propulsion (e.g. Ref. 42)

This is the author's peer reviewed, accepted manuscript. However, the online version of record will be different from this version once it has been copyedited and typeset.

PLEASE CITE THIS ARTICLE AS DOI: 10.1063/5.0134297



FIG. 1. a) Diagram of the experimental set-up inside the superconducting magnet bore. The two ultrasonic transducers are aligned along an axis, x , perpendicular to the vertical bore axis, z . Dashed lines represent the magnetic field lines. b) Image showing the 3d-printed PLA ring used to mount the transducers in the magnet bore. c) Line of eight droplets of diameters 0.4–3.0 mm (30 nL–14 μ L) levitating in the bore of the magnet, with position controlled by the acoustic-transducers.

rather than for balancing the force of gravity.

We used a custom-built 18.5 T superconducting solenoid magnet (Cryogenic Ltd., London), with a room temperature, 58 mm-diameter vertical bore, to levitate water droplets diamagnetically in air at room temperature and atmospheric pressure. The existence of a stable equilibrium levitation point for diamagnetic material in a solenoid magnet has been discussed in detail before³⁵. This point lies on the central axis, approximately 11 cm above the centre of the solenoid in our magnet, depending on the solenoid current, I . The magnetic field strength at the geometric centre of the solenoid was maintained at a constant $B_0(I) = 17.4$ T for all experiments in this letter. The bore was fitted with a custom, 3d-printed PLA ring of inner diameter 39 mm, outer diameter 57 mm and height 20 mm, see figure 1a,b. This ring contained two 10 mm diameter ultrasonic transducers (CamdenBoss CTD40K1007T), of the type used in the multi-emitter acoustic levitator, ‘TinyLev’⁴³. The transducers were positioned diametrically opposite each other and aligned along a horizontal axis such that their faces were perpendicular to the edge of the ring, as shown in figure 1. The transducers were wired in parallel, driven in-phase, and connected to a function generator (Stanford Research DS345), which was used to drive the transducers with frequencies of 37–40 kHz and up to a maximum peak-to-peak voltage, V_{pp} , of 20 V. The ring was fitted in the bore of the magnet such that the central horizontal plane of the ring intersected with the stable equilibrium levitation position of a diamagnetically levitated water droplet (fig. 1a). The sound pressure level close to the bore axis at $V_{pp} = 20$ V was ~ 110 dB, obtained from the force balance between the radial magnetic and acoustic

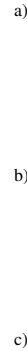


FIG. 2. a) Slice through the calculated magnetogravitational potential, $U_{mg}(x,y,z)$, in the $y = 0$ plane. The coordinates x,y,z are as defined in Fig. 1; the location of the local minimum in U_{mg} (blue circle) defines their origin. b) Slice through the calculated total potential $U_{total}(x,y,z)$, which is the sum of U_{mg} and the acoustic potential U_{acoust} , in the $y = 0$ plane. Blue circles indicate the local minima. N.b.: whereas U_{mg} is cylindrically symmetric about the z axis, U_{total} is not. c) Slice through $U_{total}(x,y,z)$ in the $z = 0$ plane. The locations of the minima closest to the bore axis lie on this plane; the others lie at slightly higher z as shown in the centre panel. The superposed photograph shows water droplets levitating at local minima in U_{total} .

forces in equilibrium, and from simulation. The operation of the transducers, despite containing some ferromagnetic material, was not affected by the presence of the strong magnetic field. Images were taken using a camera sited away from the magnet, using a 45° mirror placed several centimetres above the levitating droplets, at the mouth of the bore, to avoid influencing the acoustic field.

An atomiser was used to spray a fine mist of distilled water above the magnet, which then descended into the magnet bore. With the acoustic transducers switched off, the mist of droplets coalesced as one larger droplet at the stable levitation point. When a voltage was applied to the transducers and the experiment repeated, the mist coalesced into several well-separated droplets, each levitating in stable equilibrium. Fig-

ure 1c is a photograph, taken from an angle looking down the axis of the magnet bore, showing the formation of eight separate droplets from the mist. The droplets in this experiment have diameters in the range 0.4–3.0 mm (volume 30 nl–14 μ l), and are separated by approximately 5 mm. The two centre droplets lie approximately 2 mm from the axis of the bore. This image is representative of all experiments we performed using this method: while the sizes of the individual droplets show some variation between repeat experiments, the position and spacing between the droplets is constant for a given frequency and voltage. The technique usually produced droplets that were larger closer to the axis, since the diamagnetic force funnelled the mist toward the axis as it descended, though in principle droplets with uniform size could be levitated.

Figure 2a shows a contour plot of the magnetogravitational potential energy density U_{mg} for water in air^{35,44}

$$U_{mg} = \frac{(\chi_a - \chi_w)}{2\mu_0} B^2 - (\rho_a - \rho_w)gz, \quad (1)$$

where $\chi_w = -9.05 \times 10^{-6}$, $\chi_a = 5.13 \times 10^{-7}$, $\rho_w = 998 \text{ kg m}^{-3}$ and $\rho_a = 1.2 \text{ kg m}^{-3}$ are the volume magnetic susceptibilities (S.I. units) and densities of water (w) and air (a) respectively⁴⁵, $B(x, y, z)$ is the magnetic field strength, g is the acceleration due to gravity, μ_0 is the vacuum permeability, and z is the vertical coordinate. The terms proportional to ρ_a and χ_a account for the relatively small buoyancy of the (weakly paramagnetic) air. The magnetic field strength B was calculated from the known current density and geometry of the solenoid by numerical integration of the Biot-Savart integral. The blue circle in the figure marks the location of a local minimum in U_{mg} , i.e. the location of the stable levitation point. We take this point to be the origin of a coordinate system in which the $x - y$ plane is perpendicular to the axis, z , of the solenoid, and in which the x axis intersects the centres of the faces of both transducers (fig. 1a). The magnetic field strength at this point is $B \approx 11 \text{ T}$.

Figure 2b and c show the total potential energy density

$$U_{total} = U_{mg} + U_{acoust}, \quad (2)$$

where the acoustic potential energy density U_{acoust} of a droplet is given by the Gor'kov potential per unit volume⁴⁶

$$U_{acoust} = \frac{3}{2} \left[f_1 \frac{\langle p^2 \rangle}{3\rho_a c_a^2} - f_2 \frac{\rho_a \langle u^2 \rangle}{2} \right], \quad (3)$$

$$f_1 = 1 - \frac{\rho_a c_a^2}{\rho_w c_w^2},$$

$$f_2 = \frac{2(\rho_w - \rho_a)}{2\rho_w + \rho_a}.$$

Here, c is the speed of sound in water (w) and air (a) at room temperature and pressure respectively, and $\langle p^2 \rangle$ and $\langle u^2 \rangle$ are the mean square amplitudes of the pressure and velocity of air, respectively. For the case of water in air $f_1 \approx f_2 \approx 1$. The acoustic field inside the magnet bore was calculated using a finite-element method, implemented using the open-source software FreeFem^{47,48}, where our computational mesh was

a)
b)

FIG. 3. a) Montage of images of two levitating droplets showing the variation in their horizontal position, x , as V_{pp} was reduced from 20 V to 8 V. Down-pointing arrows indicate the voltage below which droplets lost equilibrium. b) Measured x -coordinates of the centres of the droplets. In both plots, red circles show the calculated x -coordinates of local minima in U_{total} . The blue unbroken lines indicate the x -coordinates of the two minima at $V_{pp} = 20 \text{ V}$.

generated using the open-source software Gmsh⁴⁹. More information about the method of solution and the geometry of the simulation domain used can be found in the supplementary information. The simulations show that the addition of the acoustic field modulates the potential energy density, U_{total} , giving rise to multiple potential minima, ‘wells’, along the x -axis (fig. 2b, c). Unlike U_{mg} , U_{total} is not cylindrically symmetric about the z (solenoid) axis. Figure 2b shows U_{total} in the $y = 0$ plane. Blue circles indicate the positions of each well. The two central wells lie on the x -axis, i.e. on the line passing through the centres of the two acoustic transducers. The vertical, z , location of each well increases approximately as x^4 , increasing to $z = 3 \text{ mm}$ for the wells farthest from the axis, at $|x| = 17 \text{ mm}$. This variation in height results from the shape of U_{mg} , in particular an octupole contribution to U_{mg} ⁵⁰. Figure 2c shows U_{total} in the $z = 0$ plane, and includes a photograph of levitating droplets taken from an angle looking down the bore (i.e. down the z axis), superposed on the contours.

By varying the peak-to-peak voltage V_{pp} applied to the transducers we were able to adjust the horizontal (x) positions of the levitating droplets. The montage of photographs in figure 3 shows the horizontal position of two levitated water droplets close to the solenoid axis as a function of V_{pp} . In this particular experiment, the droplet farthest from the axis had a diameter of $1.19 \pm 0.05 \text{ mm}$ and the droplet closest to the axis was larger, with a diameter of $1.93 \pm 0.05 \text{ mm}$ (the measurement uncertainty reflects the resolution of our optical set-up). Note that, since the total potential en-

ergy density, U_{total} , is independent of volume, the positions of the stable equilibrium points are independent of the volume of the droplets. When the transducers were driven with $V_{pp} = 20.0$ V, the smaller droplet levitated with its centre at $x = 7.21 \pm 0.03$ mm and the larger levitated with its centre at $x = 2.16 \pm 0.03$ mm. The levitation of both was stable. Decreasing V_{pp} from 20 V to 15 V, the position of the smaller droplet decreased from $x = 7.21$ mm to 6.85 ± 0.03 mm, while the position of the larger droplet decreased slightly from $x = 2.16$ mm to 2.06 ± 0.03 mm. On decreasing V_{pp} below 15 V, we observed that the smaller of the two droplets lost equilibrium, as the depth of the local potential well was reduced to zero, and 'fell' toward the larger of the two, coalescing with it. On decreasing V_{pp} further, from 14 V to 8 V, the equilibrium position of the centre of the remaining large droplet decreased from $x = 2.06$ mm to 1.50 ± 0.03 mm. Below $V_{pp} = 8$ V, this droplet also lost equilibrium and 'fell' radially, finding a new equilibrium on the solenoid axis. The equilibrium positions obtained from simulation and experiment are shown together in figure 3, for comparison.

The use of acoustic levitation in areas such as analytical chemistry and biochemistry is growing, where it allows analysis of small volumes of liquid without the problems associated with the presence of container walls, such as adsorption and contamination of the analyte, or measurement interference (see, e.g. Ref. 51 and references therein). Recent further strides have been taken to extend the technique to enable contactless transport and processing of multiple levitated objects, which opens up many more applications including in biochemistry, pharmaceuticals and materials science (e.g. Refs. 52 and 53). Here we have demonstrated that, by combining techniques from diamagnetic and acoustic levitation, we can trap quiescent liquid droplets with volumes $\sim 10^{-8}$ – 10^{-5} L in a series of potential wells arrayed along a horizontal line, and that the location of these traps, and thus the droplets, can be varied precisely. By lifting the drops diamagnetically, the sound pressure levels were much reduced compared to those of an acoustic levitator: ~ 110 dB compared to 150–165 dB²⁸, a greater than 100-fold reduction in the amplitude of the pressure. Consistent with this, we did not observe phenomena such as vibration of the droplets, deformation of their equilibrium shape, or instabilities in their position, which are characteristic of acoustic levitators^{22,26,30}; further experiments are planned to quantify the reduction in fluid flows within and surrounding the droplets using this set-up. We suggest that this technique may be useful in areas where particularly delicate handling of material is required, where control over the internal droplet flow is important or where evaporation and cooling by the oscillating air flow are problematic. We note that many common techniques used in biochemical analysis are compatible with a strong magnetic field, such as fluorescence microscopy⁵⁴, Raman spectroscopy⁵⁵, and light scattering⁵⁶.

The combination of acoustic and magnetic forces creates additional possibilities to manipulate the droplets: here, we demonstrated controlled contactless coalescence of two droplets by varying the ratchet-like potential U_{total} , using a

relatively simple acoustic set-up consisting of two low-power transducers, a feat that otherwise requires large transducer arrays^{52,53}. Droplets can also be moved vertically by adjusting the electric current in the solenoid. With the addition of more acoustic transducers, we anticipate that this flexibility will allow the creation of a system that can provide spatial positioning in three directions within the bore of the magnet.

SUPPLEMENTARY MATERIAL

See supplementary material for additional information about numerical simulations.

ACKNOWLEDGMENTS

We thank Dr. B. Turnbull for use of the high-resolution camera and S. Devlin for help with the design and printing of the PLA ring. This work was supported by a research grant from the Leverhulme Trust (Grant No. RPG-2018-363).

DATA AVAILABILITY STATEMENT

The data that supports the findings of this study are available within the article and its supplementary material.

AUTHOR DECLARATIONS

Conflict of Interest

The authors have no conflicts to disclose.

Author Contributions

All authors contributed equally to this work.

¹N. Leopold, M. Haberkorn, T. Laurell, J. Nilsson, J. R. Baena, J. Frank, and B. Lendl, "On-line monitoring of airborne chemistry in levitated nanodroplets: In situ synthesis and application of SERS-active Ag-sols for trace analysis by FT-Raman spectroscopy," *Anal. Chem.* **75**, 2166 (2003).

²J. Leiterer, W. Leitenberger, F. Emmerling, A. F. Thünemann, and U. Panne, "The use of an acoustic levitator to follow crystallization in small droplets by energy dispersive X-ray diffraction," *J. Appl. Crystallogr.* **39**, 771 (2006).

³M. S. Westphal, K. Jorabchi, and L. M. Smith, "Mass spectrometry of acoustically levitated droplets," *Anal. Chem.* **80**, 5847 (2008).

⁴C. Warschat, A. Stindt, U. Panne, and J. Riedel, "Mass Spectrometry of Levitated Droplets by Thermally Unconfined Infrared-Laser Desorption," *Anal. Chem.* **87**, 8323 (2015).

⁵S. Tsujino and T. Tomizaki, "Ultrasonic acoustic levitation for fast frame rate X-ray protein crystallography at room temperature," *Sci. Rep.* **6**, 1 (2016).

⁶S. J. Brotton and R. I. Kaiser, "Controlled Chemistry via Contactless Manipulation and Merging of Droplets in an Acoustic Levitator," *Anal. Chem.* **92**, 8371 (2020).

⁷J. R. Gao, C. D. Cao, and B. Wei, "Containerless processing of materials by acoustic levitation," *Adv. Space Res.* **24**, 1293 (1999).

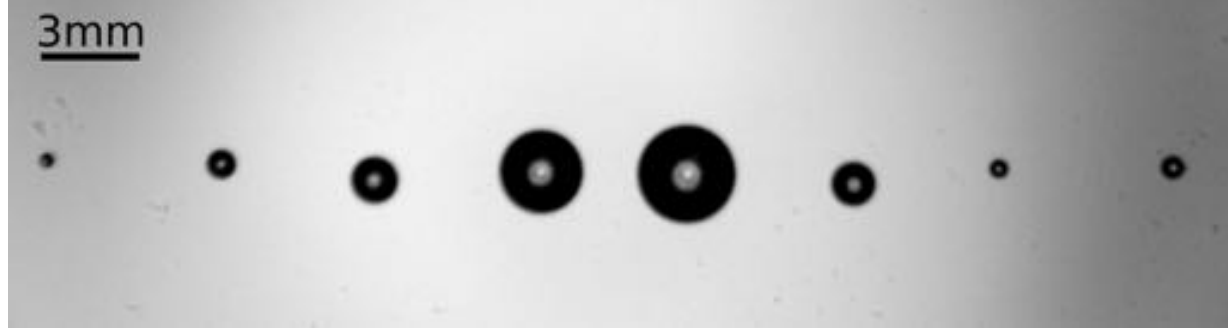
This is the author's peer reviewed, accepted manuscript. However, the online version of record will be different from this version once it has been copyedited and typeset.

PLEASE CITE THIS ARTICLE AS DOI: 10.1063/5.0134297

- ⁸C. J. Benmore and J. K. Weber, "Amorphization of Molecular Liquids of Pharmaceutical Drugs by Acoustic Levitation," *Phys. Rev. X* **1**, 1 (2011).
- ⁹C. J. Benmore, J. K. Weber, A. N. Taylor, B. R. Cherry, J. L. Yarger, Q. Mou, W. Weber, J. Neufeind, and S. R. Byrn, "Structural characterization and aging of glassy pharmaceuticals made using acoustic levitation," *J. Pharm. Sci.* **102**, 1290 (2013).
- ¹⁰V. Vandaele, P. Lambert, and A. Delchambre, "Non-contact handling in microassembly: Acoustical levitation," *Precis. Eng.* **29**, 491 (2005).
- ¹¹S. Deng, K. Jia, E. Wu, X. Hu, Z. Fan, and K. Yang, "Controllable micro-particle rotation and transportation using sound field synthesis technique," *Appl. Sci.* **8**, 73 (2018).
- ¹²M. A. Andrade, T. S. Camargo, and A. Marzo, "Automatic contactless injection, transportation, merging, and ejection of droplets with a multifocal point acoustic levitator," *Rev. Sci. Instrum.* **89**, 125105 (2018).
- ¹³I. Ezcurdia, R. Morales, M. A. B. Andrade, and A. Marzo, "LeviPrint: Contactless Fabrication Using Full Acoustic Trapping of Elongated Parts," in *ACM SIGGRAPH Conf. Proc.* **1**, 1 (2022).
- ¹⁴M. A. B. Andrade, N. Pérez, and J. C. Adamowski, "Review of Progress in Acoustic Levitation," *Braz. J. Phys.* **48**, 190 (2018).
- ¹⁵T. Hoshi, M. Takahashi, T. Iwamoto, and H. Shinoda, "Noncontact tactile display based on radiation pressure of airborne ultrasound," *IEEE Trans. Haptics* **3**, 155 (2010).
- ¹⁶T. Hoshi, Y. Ochiai, and J. Rekimoto, "Three-dimensional noncontact manipulation by opposite ultrasonic phased arrays," *Jpn. J. Appl. Phys.* **53**, 07KE07 (2014).
- ¹⁷R. H. Morris, E. R. Dye, P. Docker, and M. I. Newton, "Beyond the Langevin horn: Transducer arrays for the acoustic levitation of liquid drops," *Phys. Fluids* **31**, 101301 (2019).
- ¹⁸F. S. Lin, P. W. Yang, C. C. Hsieh, H. Y. Su, L. X. Chen, C. Y. Li, and C. H. Huang, "Investigation of a Novel Acoustic Levitation Technique Using the Transition Period Between Acoustic Pulse Trains and Electrical Driving Signals," *IEEE Trans. Ultrason. Ferroelectr. Freq. Control* **69**, 769 (2022).
- ¹⁹M. Rothlisberger, G. Schmidli, M. Schuck, and J. W. Kolar, "Multi-Frequency Acoustic Levitation and Trapping of Particles in All Degrees of Freedom," *IEEE Trans. Ultrason. Ferroelectr. Freq. Control* **69**, 1572 (2022).
- ²⁰L. Zhili, Z. Heng, P. Huiyu, Y. Mian, P. Yifan, and Z. Li, "Acoustic Levitation for Large Particle Based on Concave Spherical Transducer Arrays," *IEEE Sens. J.* **22**, 18104 (2022).
- ²¹D. Zang, Y. Yu, Z. Chen, X. Li, H. Wu, and X. Geng, "Acoustic levitation of liquid drops: Dynamics, manipulation and phase transitions," *Adv. Colloid Interface Sci.* **243**, 77 (2017).
- ²²J. Rudnick and M. Barmatz, "Oscillational instabilities in single-mode acoustic levitators," *J. Acoust. Soc. Am.* **87**, 81 (1990).
- ²³M. A. B. Andrade, N. Pérez, and J. C. Adamowski, "Experimental study of the oscillation of spheres in an acoustic levitator," *J. Acoust. Soc. Am.* **136**, 1518 (2014).
- ²⁴E. H. Trinh and J. L. Robey, "Experimental study of streaming flows associated with ultrasonic levitators," *Phys. Fluids* **6**, 3567 (1994).
- ²⁵K. Hasegawa, Y. Abe, A. Kaneko, Y. Yamamoto, and K. Aoki, "Visualization measurement of streaming flows associated with a single-acoustic levitator," *Microgravity Sci. Technol.* **21**, 9 (2009).
- ²⁶L. Cox, A. Croxford, B. W. Drinkwater, and A. Marzo, "Acoustic Lock: Position and orientation trapping of non-spherical sub-wavelength particles in mid-air using a single-axis acoustic levitator," *Appl. Phys. Lett.* **113**, 054101 (2018).
- ²⁷P. Helander, T. Puranen, A. Meriläinen, G. Maconi, A. Penttilä, M. Gritsevich, I. Kassamakov, A. Salmi, K. Muinonen, and E. Hægström, "Omnidirectional microscopy by ultrasonic sample control," *Appl. Phys. Lett.* **116**, 194101 (2020).
- ²⁸N. Kawahara, A. L. Yarin, G. Brenn, O. Kastner, and F. Durst, "Effect of acoustic streaming on the mass transfer from a sublimating sphere," *Phys. Fluids* **12**, 912 (2000).
- ²⁹A. L. Yarin, G. Brenn, O. Kastner, D. Rensink, and C. Tropea, "Evaporation of acoustically levitated droplets," *J. Fluid Mech.* **399**, 151 (1999).
- ³⁰A. L. Yarin, M. Pfaffenlehner, and C. Tropea, "On the acoustic levitation of droplets," *J. Fluid Mech.* **356**, 65 (1998).
- ³¹C. L. Shen, W. J. Xie, and B. Wei, "Parametrically excited sectorial oscillation of liquid drops floating in ultrasound," *Phys. Rev. E* **81**, 046305 (2010).
- ³²L. Liao and R. J. A. Hill, "Shapes and Fissility of Highly Charged and Rapidly Rotating Levitated Liquid Drops," *Phys. Rev. Lett.* **119**, 114501 (2017).
- ³³E. Beaugnon and R. Tournier, "Levitation of organic materials," *Nature* **349**, 470 (1991).
- ³⁴M. A. Weiler, D. L. Whitaker, H. J. Maris, and G. M. Seidel, "Magnetic levitation and noncoalescence of liquid helium," *Phys. Rev. Lett.* **77**, 4840 (1996).
- ³⁵M. V. Berry and A. K. Geim, "Of flying frogs and levitrons," *Eur. J. Phys.* **18**, 307 (1997).
- ³⁶J. M. Valles, K. Lin, J. M. Denegre, and K. L. Mowry, "Stable magnetic field gradient levitation of *Xenopus laevis*: Toward low-gravity simulation," *Biophys. J.* **73**, 1130 (1997).
- ³⁷Y. Tanimoto, M. Fujiwara, M. Sueda, K. Indue, and M. Akita, "Magnetic levitation of plastic chips: Applications for magnetic susceptibility measurement and magnetic separation," *Jpn. J. Appl. Phys.* **44**, 6801 (2005).
- ³⁸C. Lorin, A. Mailfert, D. Chatain, H. Flice, and D. Beysens, "Magnetogravitational potential revealed near a liquid-vapor critical point," *J. Appl. Phys.* **106**, 033905 (2009).
- ³⁹K. A. Baldwin, S. L. Butler, and R. J. A. Hill, "Artificial tektites: An experimental technique for capturing the shapes of spinning drops," *Sci. Rep.* **5**, 1 (2015).
- ⁴⁰S. Nakata, M. Yoshikai, Y. Gunjima, and M. Fujiwara, "Synchronized motion of two camphor disks on a water droplet levitated under microgravity," *Colloids Surf. A* **655**, 130321 (2022).
- ⁴¹M. Fujimoto and M. Koshino, "Diamagnetic levitation and thermal gradient driven motion of graphite," *Phys. Rev. B* **100**, 045405 (2019).
- ⁴²L. Xu, D. Gong, K. Chen, J. Cai, and W. Zhang, "Acoustic levitation applied for reducing undesired lateral drift of magnetic helical microrobots," *J. Appl. Phys.* **128**, 184703 (2020).
- ⁴³A. Marzo, A. Barnes, and B. W. Drinkwater, "TinyLev: A multi-emitter single-axis acoustic levitator," *Rev. Sci. Instrum.* **88**, 085105 (2017).
- ⁴⁴A. T. Catherall, P. López-Alcaraz, K. A. Benedict, P. J. King, and L. Eaves, "Cryogenically enhanced magneto-archimedes levitation," *New J. Phys.* **7**, 118 (2005).
- ⁴⁵R. S. Davis, "Equation for the volume magnetic susceptibility of moist air," *Metrologia* **35**, 49 (1998).
- ⁴⁶L. P. Gorkov, "Forces acting on a small particle in an acoustic field within an ideal fluid," *Dokl. Akad. Nauk SSSR* **140**, 88 (1961).
- ⁴⁷F. Hecht, "New development in FreeFem++," *J. Numer. Math.* **20**, 251 (2012).
- ⁴⁸J. Deakin, "Optimal PML transformations for the Helmholtz equation," The University of Manchester (United Kingdom), 2020.
- ⁴⁹C. Geuzaine and J. F. Remacle, "Gmsh: A 3-D finite element mesh generator with built-in pre- and post-processing facilities," *Int. J. Numer. Methods Eng.* **79**, 1309 (2009).
- ⁵⁰R. J. A. Hill and L. Eaves, "Vibrations of a diamagnetically levitated water droplet," *Phys. Rev. E* **81**, 056312 (2010).
- ⁵¹S. Santesson and S. Nilsson, "Airborne chemistry: Acoustic levitation in chemical analysis," *Anal. Bioanal. Chem.* **378**, 1704 (2004).
- ⁵²D. Foresti, M. Nabavi, M. Klingauf, A. Ferrari, and D. Poulikakos, "Acoustophoretic contactless transport and handling of matter in air," *Proc. Natl. Acad. Sci. U. S. A.* **110**, 12549 (2013).
- ⁵³A. Watanabe, K. Hasegawa, and Y. Abe, "Contactless fluid manipulation in air: Droplet coalescence and active mixing by acoustic levitation," *Sci. Rep.* **8**, 0 (2018).
- ⁵⁴Y. Kitahama, Y. Kimura, and K. Takazawa, "Study of internal structure of meso-tetrakis (4-Sulfonatophenyl) porphine J-aggregates in solution by fluorescence microscope imaging in a magnetic field," *Langmuir* **22**, 7600 (2006).
- ⁵⁵J. A. Perenboom, S. A. Wieggers, P. C. M. Christianen, U. Zeitler, and J. C. Maan, "Research in high magnetic fields: The installation at the University of Nijmegen," *J. Low Temp. Phys.* **133**, 181 (2003).
- ⁵⁶P. G. Van Rhee, R. S. Rikken, L. K. Abdelmohsen, J. C. Maan, R. J. Nolte, J. C. Van Hest, P. C. M. Christianen, and D. A. Wilson, "Polymersome magneto-valves for reversible capture and release of nanoparticles," *Nat. Commun.* **5**, 5010 (2014).

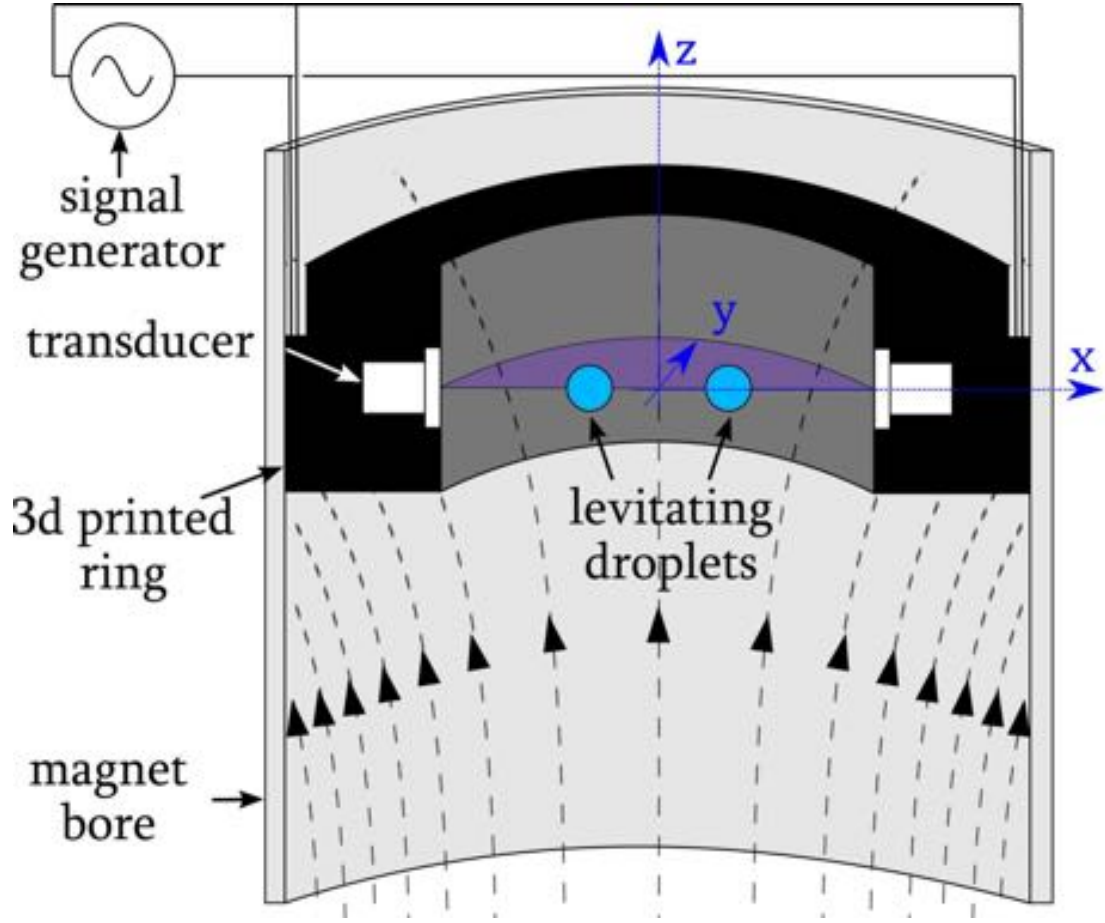
This is the author's peer reviewed, accepted manuscript. However, the online version of record will be different from this version once it has been copyedited and typeset.

PLEASE CITE THIS ARTICLE AS DOI: 10.1063/1.50134297



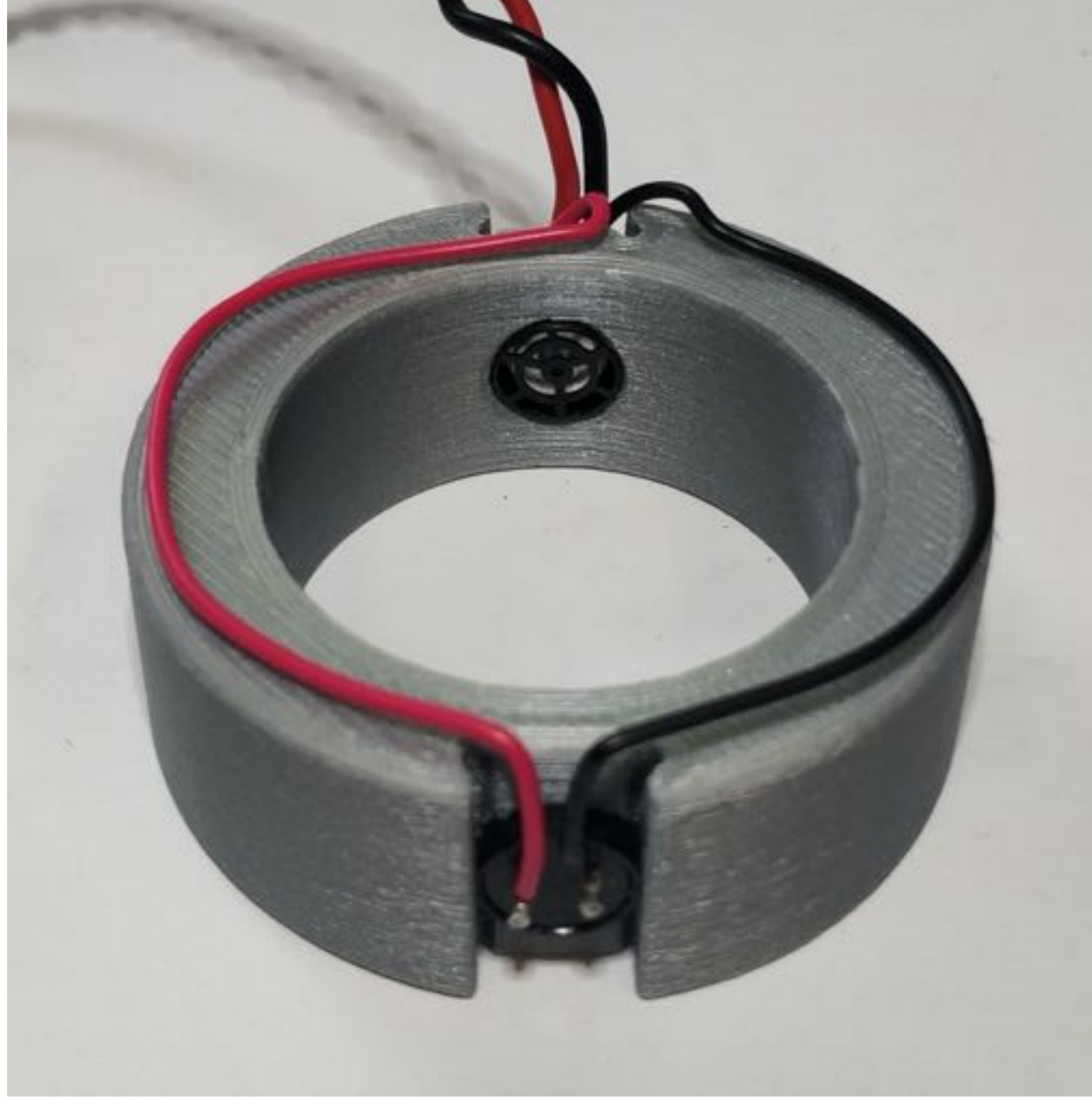
This is the author's peer reviewed, accepted manuscript. However, the online version of record will be different from this version once it has been copyedited and typeset.

PLEASE CITE THIS ARTICLE AS DOI: 10.1063/1.50134297



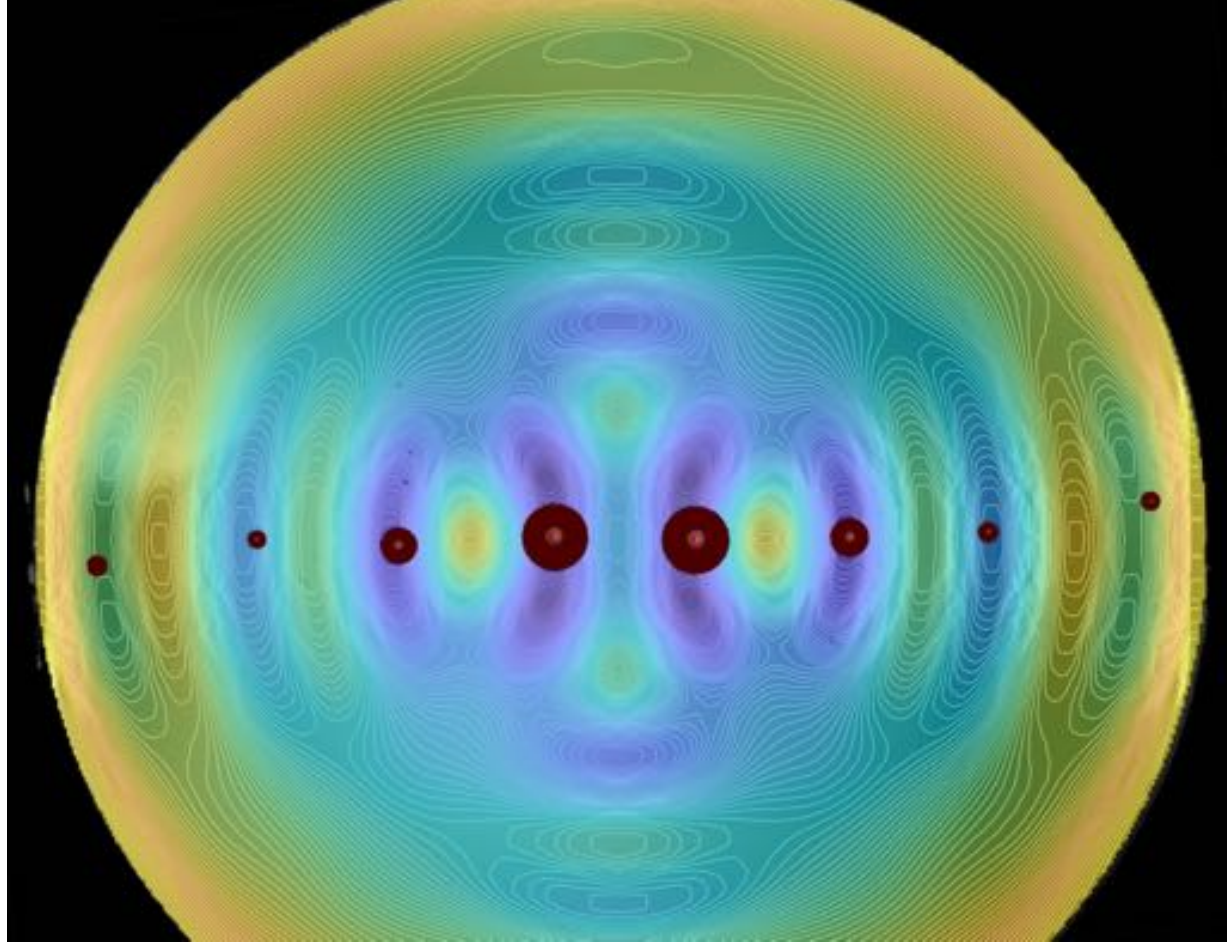
This is the author's peer reviewed, accepted manuscript. However, the online version of record will be different from this version once it has been copyedited and typeset.

PLEASE CITE THIS ARTICLE AS DOI: 10.1063/1.50134297



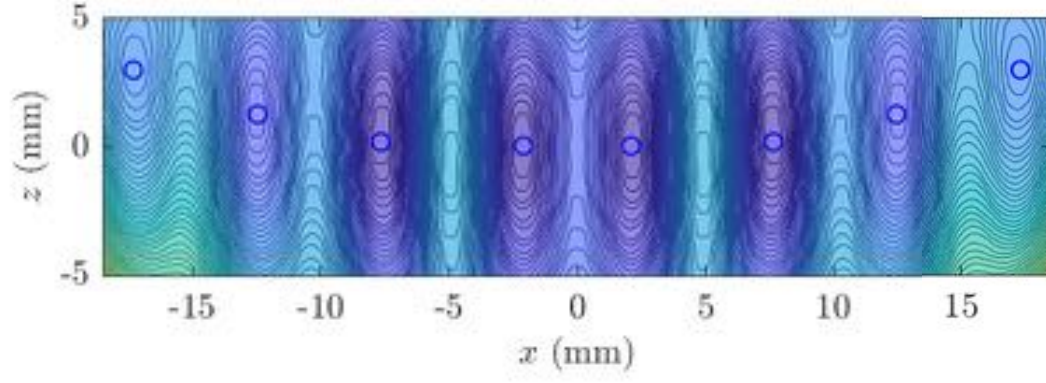
This is the author's peer reviewed, accepted manuscript. However, the online version of record will be different from this version once it has been copyedited and typeset.

PLEASE CITE THIS ARTICLE AS DOI: 10.1063/5.0134297

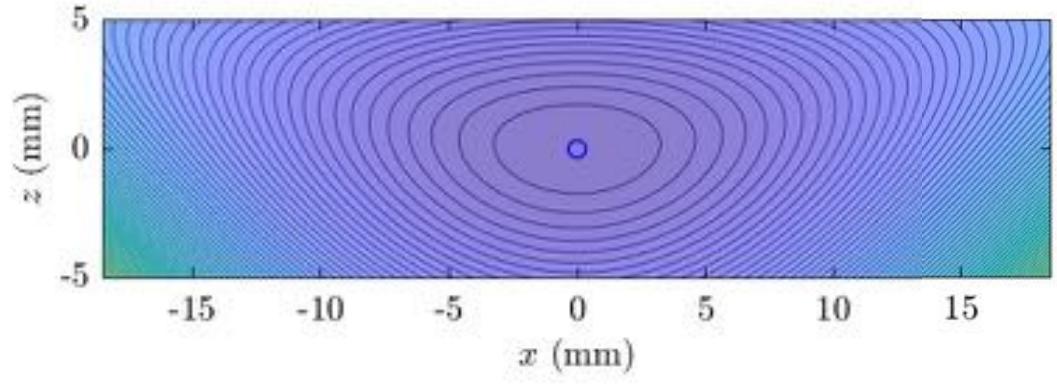


This is the author's peer reviewed, accepted manuscript. However, the online version of record will be different from this version once it has been copyedited and typeset.

PLEASE CITE THIS ARTICLE AS DOI: 10.1063/5.0134297



This is the author's peer reviewed, accepted manuscript. However, the online version of record will be different from this version once it has been copyedited and typeset.
PLEASE CITE THIS ARTICLE AS DOI: 10.1063/1.50134297



This is the author's peer reviewed, accepted manuscript. However, the online version of record will be different from this version once it has been copyedited and typeset.

PLEASE CITE THIS ARTICLE AS DOI: 10.1063/1.50134297

